

Dark Matter Freeze-out via Catalyzed Annihilation

Chuan-Yang Xing^{1,*} and Shou-hua Zhu^{1,2,3,†}

¹Department of Physics and State Key Laboratory of Nuclear Physics and Technology, Peking University, Beijing 100871, China

²Collaborative Innovation Center of Quantum Matter, Beijing, 100871, China

³Center for High Energy Physics, Peking University, Beijing 100871, China

We present a new paradigm of dark matter freeze-out, where the annihilation of dark matter particles is catalyzed. We discuss in detail the regime that the depletion of dark matter proceeds via $2\chi \rightarrow 2A'$ and $3A' \rightarrow 2\chi$ processes, in which χ and A' denote dark matter and the catalyst respectively. In this regime, the dark matter number density is depleted polynomially rather than exponentially (Boltzmann suppression) as in classic WIMPs and SIMPs. The paradigm applies for a secluded weakly interacting dark sector with a dark matter in the MeV-TeV mass range. The catalyzed annihilation paradigm is compatible with CMB and BBN constraints, with enhanced indirect detection signals.

I. Introduction

The nature of dark matter (DM) is still unknown. Though, the observed abundance of DM may give some hints on its coupling with other particles, especially Standard Model (SM) particles. For thermal DM, in the early universe, if DM is very weakly coupled and decouples from the thermal bath while relativistic, it should be rather light to reproduce the observed relic abundance, $m_{\text{DM}} \sim 6\text{eV} \frac{\Omega h^2}{0.12}$, which is not favoured [1–3]. For heavier DM, there has to be some DM depletion processes that are intense enough to freeze-out at late times so that DM is not over-produced. This motivates the studies and experimental detection of mechanisms of dark matter freeze-out.

There are essentially two kinds of process leading to depletion of DM particles in the literature. The first one is that DM particles annihilate into other particles, mostly thermal bath particles. The other one is via number-changing process. For the former case, the most studied scenario is self-annihilation process [4]. Especially, weakly interacting massive particles (WIMPs) that naturally reproduce correct relic abundance attracted extensive attentions [5–7]. Other variations on this include co-annihilation [8–10], forbidden annihilation [8, 11], semi-annihilation [12], secluded annihilation [13, 14] and so on [15–23]. Whereas, for the number-changing process, the most studied process is $3\text{DM} \rightarrow 2\text{DM}$ annihilation, dubbed as strongly interaction massive particles (SIMPs) [24, 25]. Subsequently, other number-changing process are proposed and discussed, including Z_2 -symmetric SIMPs [26, 27], co-SIMPs [28], etc.

In this work, we propose a novel kind of process of dark matter burning in the early universe. Consider a nearly secluded dark sector with a stable DM (denoted as χ in this work) and a mediator (denoted as A'). The two processes that lead to the depletion of DM are $2\chi \rightarrow 2A'$ and $3A' \rightarrow 2\chi$. We shown in Figure 1 a depiction of

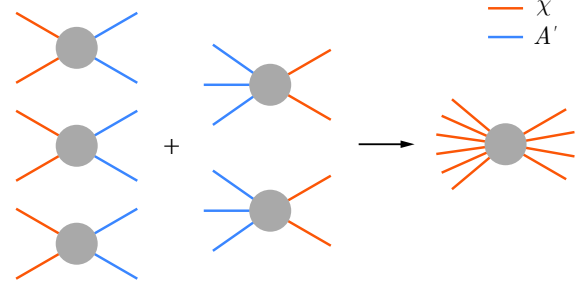


FIG. 1. Schematic illustration of the catalyzed annihilation of DM χ (red line) with a catalyst A' (blue line). Three $2\chi \rightarrow 2A'$ processes plus two $3A' \rightarrow 2\chi$ processes effectively deplete the number of dark matter particles by two.

how these annihilation channels result in depopulation of DM particles, that is, three $2\chi \rightarrow 2A'$ processes together with two $3A' \rightarrow 2\chi$ effectively deplete two dark matter particles. On the other hand, these two processes merely change the comoving number density of the mediator during the period that they dominate DM burning. The mediator acts similar to a catalyst in a chemical reaction and we dub the processes as *catalyzed annihilation* of dark matter. We acknowledge that catalyzed processes are also considered in the Big Bang Nucleosynthesis (BBN) [29] and nuclear fusion [30, 31].

In order for this paradigm to work, there are several requirements listed as follows:

- The dark sector is nearly secluded.
- The catalyst is long-lived ($\gtrsim 10^{-9}\text{s}$).
- The catalyst is slightly lighter than DM ($1 < m_\chi/m_{A'} \lesssim 2$).
- Annihilation channels as in Figure 1.

The dark sector should be secluded so that the annihilation channels to SM particles freeze-out before the catalyzed annihilation. We expect the catalyst to decay after the catalyzed annihilation freezes-out. Thus, during

* cyxing@pku.edu.cn

† shzhu@pku.edu.cn

the catalyzed annihilation, the catalyst is abundant in the primordial plasma (much more abundant than DM since $m_\chi > m_{A'}$), so that the rate of the $3A' \rightarrow 2\chi$ process is enhanced. If the catalyst decays fast, the paradigm recovers to the secluded DM regime [13, 14]. The catalyzed annihilation will heat up the dark sector. For simplicity, in this work, we assume the dark sector could scatter with SM particles intensely enough to maintain thermal equilibrium with the thermal bath.

The freeze-out mechanism of the catalyzed annihilation is unique. Different with paradigms of WIMPs and SIMPs, where the number density of DM tracks Boltzmann distribution and shrinks exponentially before freeze-out, the catalyzed annihilation could lead to a polynomial suppression of the dark matter number density n_χ as the universe cools down (see in Eq. 5 below),

$$n_\chi \propto s^{3/2} \propto x^{-9/2}, \quad (1)$$

where $x \equiv m_\chi/T$ and T is the temperature of the universe. s denotes entropy density of the thermal bath. Therefore, the catalyzed annihilation lasts longer and freezes-out at late times,

$$x_f \equiv m_\chi/T_f \simeq 800, \quad (2)$$

where T_f denotes the freeze-out temperature. To reproduce correct relic abundance, the cross section of DM annihilation $2\chi \rightarrow 2A'$ should be enhanced since there is less time to redshift to today [17]. Phenomenologically, the enhanced annihilation of DM corresponds to enhanced indirect detection signals.

II. Catalyzed Freeze-out

We show in Figure 2 a typical thermal history of DM that freezes-out via catalyzed annihilation in the early universe. For now, we are focused on the regime that the mass ratio of DM and the catalyst $r \equiv m_\chi/m_{A'}$ is no larger than 1.5. As is shown in the figure, there are essentially four stages in the thermal history of DM:

1. *Equilibrium stage.* Both DM and the catalyst A' stay in chemical equilibrium with the thermal bath.

$$n_\chi \simeq \bar{n}_\chi, n_{A'} \simeq \bar{n}_{A'}. \quad (3)$$

$n_{\chi, A'}$ denote the number densities and $\bar{n}_{\chi, A'}$ are the equilibrium densities of DM and A' with zero chemical potential. In the non-relativistic limit, we have $\bar{n}_{\chi, A'} = g_{\chi, A'} \left(\frac{m_{\chi, A'} T}{2\pi} \right)^{3/2} e^{-m_{\chi, A'}/T}$ [32], where g denotes number of internal degrees of freedom.

2. *Chemical stage.* During this period, though DM and the catalyst are chemically decoupled from the thermal bath, they can still maintain chemical equilibrium with each other via the $2\chi \leftrightarrow 2A'$ process.

$$n_\chi/\bar{n}_\chi \simeq n_{A'}/\bar{n}_{A'}. \quad (4)$$

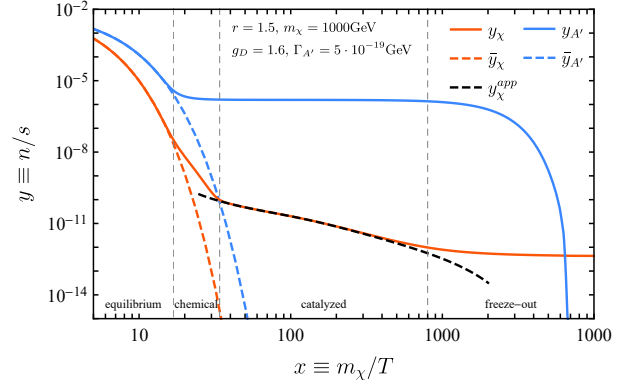


FIG. 2. Thermal evolution of DM (solid red) and the catalyst (solid blue). The dashed curves denote equilibrium yields for DM and the catalyst respectively, while the dashed black curve shows the approximate DM number density during the catalyzed annihilation stage $n_\chi^{app} = \sqrt{n_{A'}^3 \langle \sigma_3 v^2 \rangle / \langle \sigma_2 v \rangle}$ from Eq. 5. The parameters are taken for the model presented in Section IV.

3. *Catalyzed annihilation.* After the chemical decoupling of DM and the catalyst, the catalyzed annihilation takes over. In this stage, the $3A' \rightarrow 2\chi$ process dominates over $2A' \rightarrow 2\chi$ annihilation since the latter is exponentially suppressed at low temperature. The rate of $3A' \rightarrow 2\chi$ process turns comparable with the $2\chi \rightarrow 2A'$ annihilation rate.

$$\langle \sigma_2 v \rangle n_\chi^2 \simeq \langle \sigma_3 v^2 \rangle n_{A'}^3. \quad (5)$$

We used $\langle \sigma_2 v \rangle$ and $\langle \sigma_3 v^2 \rangle$ to denote the thermally averaged cross section of $2\chi \rightarrow 2A'$ and $3A' \rightarrow 2\chi$ processes respectively.

4. *Freeze-out and the catalyst decays.* As the universe expands, the rate of the catalyzed annihilation descends and freezes-out. The catalyst is expected to decay after the freeze-out.

The equilibrium stage ends when the rates of the number-changing processes inside the dark sector fall behind the expansion of the universe. The dominate number-changing process is $3A' \rightarrow 2\chi$ for moderately large mass ratio $r \gtrsim 1.1$, since the catalyst is exponentially more abundant than DM at low temperature $n_{A'} \gg n_\chi$. Other processes with DM in the initial state, e.g. $\chi A' A' \rightarrow \chi A'$, are suppressed and negligible. Subsequently, we can determine the temperature of departure from equilibrium T_c approximately,

$$\langle \sigma_3 v^2 \rangle n_{A'}^3 \simeq H(n_{A'} + n_\chi), \quad (6)$$

where H is Hubble constant. We note that the annihilation channels to SM particles or the $3A' \rightarrow 2A'$ process can also result in depletion of dark sector particles. The departure from equilibrium could be determined by these channels if they freeze-out later. Similarly, the catalyzed

annihilation freezes-out when the rate drops below Hubble constant. The freeze-out temperature T_f , therefore, is determined by,

$$\langle \sigma_2 v \rangle n_\chi^2 \simeq \langle \sigma_3 v^2 \rangle n_{A'}^3 \simeq H n_\chi. \quad (7)$$

Note the difference between Eq. 6 and Eq. 7.

The relic abundance of DM can be estimated approximately in the same spirit of WIMPs [33],

$$\Omega_\chi = \frac{m_\chi s_0 H_m}{\rho_c s_m} \frac{\sqrt{g_{*,m}}}{\sqrt{g_{*,f}}} \frac{x_f}{\langle \sigma_2 v \rangle}, \quad (8)$$

where $x_f \equiv m_\chi/T_f$. The subscripts m and f mark the temperatures, $T = m_\chi$ and $T = T_f$ respectively, for the quantities, including entropy density s , Hubble constant H and effective degrees of freedom g_* ¹. ρ_c denotes critical energy density and s_0 is the entropy density today. We emphasize that although T_c deduced from Eq. 6 does not show explicitly in Eq. 8, the freeze-out temperature T_f is dependent on T_c and DM relic abundance changes if the departure from equilibrium is delayed due to annihilation channels to SM particles or $3A' \rightarrow 2A'$ process.

Based on the partial wave unitarity limit [34], $\sigma_2 v \leq \frac{4\pi}{m_\chi^2 v}$, we can estimate the upper bound of DM mass from Eq. 8 for the catalyzed annihilation paradigm. With $x_f \gtrsim 100$, we deduce,

$$m_\chi \lesssim 100 \text{TeV}. \quad (9)$$

Compared to SIMP dark matter that lives in MeV scale [24], it is intriguing to notice that $3 \rightarrow 2$ process can apply to such a heavy dark matter.

In order to study the thermal evolution and DM freeze-out in a quantitative way, we turn to the Boltzmann equations. As is discussed above, we neglect the subdominant $3 \rightarrow 2$ annihilation channels, including $\chi A' A' \rightarrow \chi A'$, $\chi \chi A' \rightarrow A' A'$, $\chi \chi A' \rightarrow \chi \chi$, $\chi \chi \chi \rightarrow \chi A'$ and assume $3A' \rightarrow 2A'$ is subdominant. If A' decays to SM particles, the Boltzmann equations reads,

$$\begin{aligned} \dot{n}_\chi + 3H n_\chi &= -2 \langle \sigma_2 v \rangle \left(n_\chi^2 - \bar{n}_\chi^2 \frac{n_{A'}^2}{\bar{n}_{A'}^2} \right) \\ &\quad + 2 \langle \sigma_3 v^2 \rangle \left(n_{A'}^3 - \bar{n}_{A'}^3 \frac{n_\chi^2}{\bar{n}_\chi^2} \right), \\ \dot{n}_{A'} + 3H n_{A'} &= +2 \langle \sigma_2 v \rangle \left(n_\chi^2 - \bar{n}_\chi^2 \frac{n_{A'}^2}{\bar{n}_{A'}^2} \right) \\ &\quad - 3 \langle \sigma_3 v^2 \rangle \left(n_{A'}^3 - \bar{n}_{A'}^3 \frac{n_\chi^2}{\bar{n}_\chi^2} \right) - \langle \Gamma_{A'} \rangle (n_{A'} - \bar{n}_{A'}). \end{aligned} \quad (10)$$

Note the conventions adopted in Eq. 10. We only show the number of difference in the initial and final state for

¹ We neglect the differences between effective entropy degrees of freedom $g_{*,s}$ and effective energy degrees of freedom g_* as in Ref. [17]

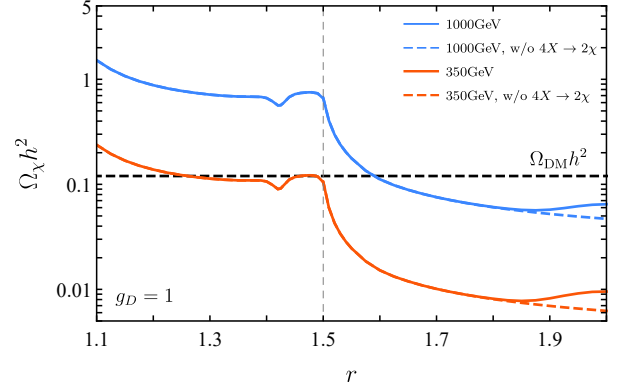


FIG. 3. Curves of relic abundance $\Omega_\chi h^2$ for $m_\chi = 350 \text{GeV}$ (solid red) and $m_\chi = 1000 \text{GeV}$ (solid blue) with respect to different mass ratio. For dashed colored curves, the $4A' \rightarrow 2\chi$ process is neglected. The dashed black curve denotes the observed DM relic abundance [36]. The parameters are taken for the model presented in Section IV.

each particle, i.e. the number of host particle for each equation in the final state minus that in the initial state. Other factors, including the initial state symmetry factor and a factor 2 if the process is not self-conjugate, are absorbed in the definition of thermal average [23, 35]. The yield of DM and the catalyst $y_{\chi, A'} \equiv n_{\chi, A'}/s$ can be solved numerically and are shown in Figure 2.

III. Mass Ratio

In previous section, we concentrated on the mass ratio $r \leq 1.5$. In fact, the catalyzed annihilation paradigm can go beyond this limit. Firstly, when the mass ratio is slightly larger than 1.5, i.e. $3m_{A'} \leq 2m_\chi$, $\langle \sigma_3 v^2 \rangle$ is exponentially suppressed as the temperature goes down,

$$\langle \sigma_3 v^2 \rangle \propto e^{-(2r-3)x/r}. \quad (11)$$

During the catalyzed annihilation period, with less DM particles produced via $3A' \rightarrow 2\chi$ process since the cross section is smaller, the number density of DM shrinks more sharply (see in Eq. 5). Consequently, the catalyzed annihilation freezes-out earlier, much earlier than the regime of $r \leq 1.5$.

As the mass ratio grows, when $r \lesssim 2$, it is intriguing to notice that the $4A' \rightarrow 2\chi$ process may play a part in the catalyzed annihilation. To be specific, after a period of catalyzed annihilation governed by the $2\chi \rightarrow 2A'$ and $3A' \rightarrow 2\chi$ processes as usual, since the $3A' \rightarrow 2\chi$ annihilation is exponentially suppressed, the non-suppressed $4A' \rightarrow 2\chi$ process takes over the role of converting the catalyst to DM particles and there would be an extra stage of catalyzed annihilation predominated by the $2\chi \rightarrow 2A'$ and $4A' \rightarrow 2\chi$ processes. Similar to Eq. 5, we can deduce an approximate relation that holds in this stage,

$$\langle \sigma_2 v \rangle n_\chi^2 \simeq \langle \sigma_4 v^3 \rangle n_{A'}^4, \quad (12)$$

where $\langle\sigma_4 v^3\rangle$ denotes the thermally averaged cross section for $4A' \rightarrow 2\chi$ process. The thermal evolution and relic abundance of DM can be significantly modified due to the $4A' \rightarrow 2\chi$ process. Specifically, if the $4A' \rightarrow 2\chi$ process is neglected, as is discussed previously, n_χ decreases exponentially (Eq. 11) during the catalyzed annihilation and freezes-out early. Once the $4A' \rightarrow 2\chi$ process takes charge, the exponentially falling of n_χ is bent and the polynomial suppression recovers (compared to Eq. 1).

$$n_\chi \propto s^2 \propto x^{-6}. \quad (13)$$

Therefore, the catalyzed annihilation freezes-out at later times, leading to an enhanced relic abundance of DM.

For even larger mass ratio, we expect the processes with more catalyst annihilating to two DM particles, e.g. $5A' \rightarrow 2\chi$, to possibly play a role in the catalyzed annihilation, especially when the dark sector is strongly coupled.

We show in Figure 3 the variation of relic abundance of DM $\Omega_\chi h^2$ with different mass ratio. When the mass ratio passes the critical value of 1.5, $\Omega_\chi h^2$ decreases rapidly. On the other hand, for $r \lesssim 2$, relic abundance is uplifted if $4A' \rightarrow 2\chi$ process is included.

IV. A Model

The requirements for realization of the catalyzed annihilation presented in Section I can be easily met in various kinds of models. In this section, we simply present a dark photon model [37–41] with a Dirac fermion χ charged under a novel $U(1)'$ gauge group and A' being the gauge field. The Lagrangian for the dark sector is,

$$\mathcal{L}_{\text{DS}} = -\frac{1}{4}F'_{\mu\nu}F'^{\mu\nu} + \frac{1}{2}m_{A'}^2 A'_\mu A'^\mu + \bar{\chi}(i\mathcal{D} - m_\chi)\chi, \quad (14)$$

where $\mathcal{D} = \not{\partial} - ig_D \not{A}'$ and g_D is the gauge coupling constant. The mass of the dark photon can be generated via the Higgs mechanism (or Stueckelberg mechanism [42, 43]). We assume the dark Higgs boson is heavy and can be integrated out. SM particles are neutral under the $U(1)'$ gauge group. Though, the dark photon can be kinetically mixed with SM hypercharge field.

$$\mathcal{L}_{\text{mix}} = -\frac{\epsilon}{2\cos\theta_W}F'_{\mu\nu}B^{\mu\nu}. \quad (15)$$

ϵ is the mixing constant and θ_W denotes the Weinberg angle. B^μ is SM hypercharge field. Therefore, the dark sector can communicate with SM particles via the mixing and the dark photon A' can decay to SM particles. We expect that the mixing constant ϵ is small so that the dark photon is long-lived and acts as the catalyst. We note that since the catalyzed annihilation happens within the dark sector, the thermal evolution of DM is generally independent of ϵ as long as it is small enough so that the dark photon decays after the freeze-out. In contrast, if the dark photon decays fast, the models recovers the

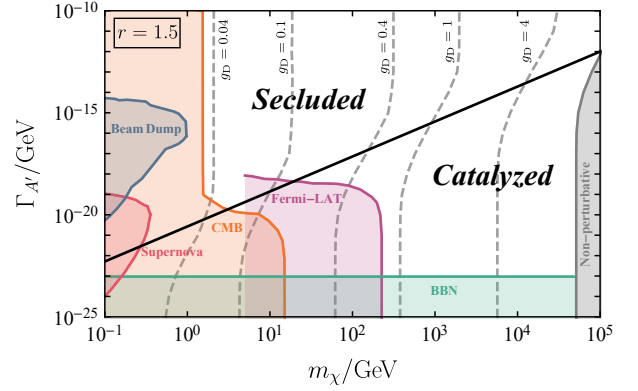


FIG. 4. Phase diagram and constraints for the dark photon model in the $(m_\chi, \Gamma_{A'})$ plane with $r = 1.5$. The solid black curve marks the boundary of the secluded phase and the catalyzed phase of the model. Correct relic abundance can be reproduced for each point in the figure by varying the value of g_D . Especially, we show in gray dashed curves for five different values of g_D that reproduce correct relic density. The non-perturbative region is painted gray, while the color-shaded regions denote the bounds from various experiments and observations correspondingly.

secluded dark matter paradigm. Additionally, we note that the kinetic mixing in Eq. 15 could not keep the dark sector in thermal equilibrium with the thermal bath since ϵ is too small. In order to thermalize the dark sector, we need another portal for the dark sector to interact with SM particles, which might be the dark Higgs. Anyhow, we won't model this part in this work and simply assume that the dark sector stays in thermal equilibrium before freeze-out.

We show in Figure 4 different phases for the model in the calculation of DM relic abundance. For short-lived dark photon, before dark matter freezes-out, it simply stays in equilibrium with the thermal bath via the decay and inverse-decay process. Thus, when DM particles annihilates into the dark photon, it immediately decays into SM particles. This is the secluded phase of the model. On the other hand, when the dark photon width $\Gamma_{A'}$ is small, the catalyzed annihilation emerges. It is a continuous shift, since the decay of the dark photon can occur during the catalyzed annihilation stage. When the dark photon decays after DM freeze-out, $\Omega_\chi h^2$ is independent with $\Gamma_{A'}$. Figure 4 shows such a feature explicitly. We show in dashed gray curves for five different values of g_D that reproduce the observed relic abundance and the curves only bend near the phase boundary.

The catalyzed annihilation paradigm is constrained by numerous terrestrial and celestial experiments and observations. Generally speaking, for any model that undergoes a period of catalyzed annihilation, the residual annihilation of DM into the catalyst after freeze-out will distort the anisotropy of the Cosmic Microwave Background (CMB) if the decay products of the catalyst are electrically charged particles [44–49]. Similarly, the signal

of the annihilation of DM at present is detectable in indirect detection experiments [50–55]. We used bounds from Fermi-LAT experiment to constrain our model in Figure 4. The late time decay of the catalyst, on the other hand, is also stringently constrained by CMB [56–58] as well as BBN [59–61]. For the dark photon model presented previously, the lower bound of the decay width of the dark photon is taken conservatively according to Ref. [61],

$$\Gamma_{A'} \geq 9.4 \cdot 10^{-24} \text{GeV}. \quad (16)$$

We note that this bound can be evaded if the catalyst decays into neutrinos or dark radiations [62–64].

For light dark photon, beam dump and fixed target experiments provide great sensitivity on the mixing coupling constant ϵ [65–68]. There are also lots of new experiments [69–72] proposed in recent years that are focused on long-lived particles. Besides, the long-lived dark photon can enhance the cooling of supernova and the constraints from SN 1987A [73–75] is widely discussed. These bounds on the dark photon model are considered and presented in Figure 4.

V. Conclusion and discussion

We proposed a novel paradigm for thermal relic dark matter, yielding the observed relic abundance. The dis-

tinctive feature of the paradigm is that the dark matter freeze-out proceeds via catalyzed annihilation. We discussed in detail the scenario that the catalyzed annihilation includes $2\chi \rightarrow 2A'$ and $3A' \rightarrow 2\chi$ processes, where χ and A' are dark matter and the catalyst respectively. The paradigm applies for a wide range of dark matter, from MeV-scale to several tens of TeV.

In this work, the dark sector is assumed to be in thermal equilibrium before freeze-out. Whereas, we note that thermal decoupling effects can significantly modify dark matter relic abundance [18, 76–80]. In fact, it can be subtle to tune the annihilation of dark sector to SM particles to be small and the thermal scattering between them to be large simultaneously, especially when the freeze-out occurs at late time. We leave this to future works [81].

Acknowledgments

C.Y.X. would like to thank Yan-Fang Bai for encouragement. This work is supported in part by the National Science Foundation of China under Grants No. 11635001, 11875072.

-
- [1] Matteo Viel, George D. Becker, James S. Bolton, and Martin G. Haehnelt, “Warm dark matter as a solution to the small scale crisis: New constraints from high redshift Lyman- α forest data,” *Phys. Rev. D* **88**, 043502 (2013), [arXiv:1306.2314 \[astro-ph.CO\]](#).
 - [2] Mohammadtaher Safarzadeh, Evan Scannapieco, and Arif Babul, “A limit on the warm dark matter particle mass from the redshifted 21 cm absorption line,” *Astrophys. J. Lett.* **859**, L18 (2018), [arXiv:1803.08039 \[astro-ph.CO\]](#).
 - [3] Nilanjan Banik, Jo Bovy, Gianfranco Bertone, Denis Erkal, and T. J. L. de Boer, “Novel constraints on the particle nature of dark matter from stellar streams,” (2019), [arXiv:1911.02663 \[astro-ph.GA\]](#).
 - [4] Benjamin W. Lee and Steven Weinberg, “Cosmological Lower Bound on Heavy Neutrino Masses,” *Phys. Rev. Lett.* **39**, 165–168 (1977).
 - [5] Gianfranco Bertone, Dan Hooper, and Joseph Silk, “Particle dark matter: Evidence, candidates and constraints,” *Phys. Rept.* **405**, 279–390 (2005), [arXiv:hep-ph/0404175](#).
 - [6] Giorgio Arcadi, Maíra Dutra, Pradipta Ghosh, Manfred Lindner, Yann Mambrini, Mathias Pierre, Stefano Profumo, and Farinaldo S. Queiroz, “The waning of the WIMP? A review of models, searches, and constraints,” *Eur. Phys. J. C* **78**, 203 (2018), [arXiv:1703.07364 \[hep-ph\]](#).
 - [7] Leszek Roszkowski, Enrico Maria Sessolo, and Sebastian Trojanowski, “WIMP dark matter candidates and searches—current status and future prospects,” *Rept. Prog. Phys.* **81**, 066201 (2018), [arXiv:1707.06277 \[hep-ph\]](#).
 - [8] Kim Griest and David Seckel, “Three exceptions in the calculation of relic abundances,” *Phys. Rev. D* **43**, 3191–3203 (1991).
 - [9] John R. Ellis, Toby Falk, and Keith A. Olive, “Neutralino - Stau coannihilation and the cosmological upper limit on the mass of the lightest supersymmetric particle,” *Phys. Lett. B* **444**, 367–372 (1998), [arXiv:hep-ph/9810360](#).
 - [10] Raffaele Tito D’Agnolo, Cristina Mondino, Joshua T. Ruderman, and Po-Jen Wang, “Exponentially Light Dark Matter from Coannihilation,” *JHEP* **08**, 079 (2018), [arXiv:1803.02901 \[hep-ph\]](#).
 - [11] Raffaele Tito D’Agnolo and Joshua T. Ruderman, “Light Dark Matter from Forbidden Channels,” *Phys. Rev. Lett.* **115**, 061301 (2015), [arXiv:1505.07107 \[hep-ph\]](#).
 - [12] Francesco D’Eramo and Jesse Thaler, “Semi-annihilation of Dark Matter,” *JHEP* **06**, 109 (2010), [arXiv:1003.5912 \[hep-ph\]](#).
 - [13] Maxim Pospelov, Adam Ritz, and Mikhail B. Voloshin, “Secluded WIMP Dark Matter,” *Phys. Lett. B* **662**, 53–61 (2008), [arXiv:0711.4866 \[hep-ph\]](#).
 - [14] Nima Arkani-Hamed, Douglas P. Finkbeiner, Tracy R. Slatyer, and Neal Weiner, “A Theory of Dark Matter,” *Phys. Rev. D* **79**, 015014 (2009), [arXiv:0810.0713 \[hep-ph\]](#).
 - [15] Jonathan L. Feng and Jason Kumar, “The WIMPless Miracle: Dark-Matter Particles without Weak-Scale Masses or Weak Interactions,” *Phys. Rev. Lett.* **101**, 231301 (2008), [arXiv:0803.4196 \[hep-ph\]](#).

- [16] Genevieve Belanger and Jong-Chul Park, “Assisted freeze-out,” *JCAP* **03**, 038 (2012), [arXiv:1112.4491 \[hep-ph\]](#).
- [17] Jeff Asaf Dror, Eric Kuflik, and Wee Hao Ng, “Codecaying Dark Matter,” *Phys. Rev. Lett.* **117**, 211801 (2016), [arXiv:1607.03110 \[hep-ph\]](#).
- [18] Raffaele Tito D’Agnolo, Duccio Pappadopulo, and Joshua T. Ruderman, “Fourth Exception in the Calculation of Relic Abundances,” *Phys. Rev. Lett.* **119**, 061102 (2017), [arXiv:1705.08450 \[hep-ph\]](#).
- [19] Mathias Garny, Jan Heisig, Marco Huftnagel, Benedikt Lülfi, and Stefan Vogl, “Conversion-driven freeze-out: Dark matter genesis beyond the WIMP paradigm,” *PoS CORFU2018*, 092 (2019), [arXiv:1904.00238 \[hep-ph\]](#).
- [20] Tarak Nath Maity and Tirtha Sankar Ray, “Exchange driven freeze out of dark matter,” *Phys. Rev. D* **101**, 103013 (2020), [arXiv:1908.10343 \[hep-ph\]](#).
- [21] Eric David Kramer, Eric Kuflik, Noam Levi, Nadav Joseph Outmezguine, and Joshua T. Ruderman, “Heavy Thermal Relics from Zombie Collisions,” (2020), [arXiv:2003.04900 \[hep-ph\]](#).
- [22] Ujjal Kumar Dey, Tarak Nath Maity, and Tirtha Sankar Ray, “Light Dark Matter through Assisted Annihilation,” *JCAP* **03**, 045 (2017), [arXiv:1612.09074 \[hep-ph\]](#).
- [23] James M. Cline, Hongwan Liu, Tracy Slatyer, and Wei Xue, “Enabling Forbidden Dark Matter,” *Phys. Rev. D* **96**, 083521 (2017), [arXiv:1702.07716 \[hep-ph\]](#).
- [24] Yonit Hochberg, Eric Kuflik, Tomer Volansky, and Jay G. Wacker, “Mechanism for Thermal Relic Dark Matter of Strongly Interacting Massive Particles,” *Phys. Rev. Lett.* **113**, 171301 (2014), [arXiv:1402.5143 \[hep-ph\]](#).
- [25] Yonit Hochberg, Eric Kuflik, Hitoshi Murayama, Tomer Volansky, and Jay G. Wacker, “Model for Thermal Relic Dark Matter of Strongly Interacting Massive Particles,” *Phys. Rev. Lett.* **115**, 021301 (2015), [arXiv:1411.3727 \[hep-ph\]](#).
- [26] Nicolas Bernal and Xiaoyong Chu, “ Z_2 SIMP Dark Matter,” *JCAP* **01**, 006 (2016), [arXiv:1510.08527 \[hep-ph\]](#).
- [27] Nicolás Bernal, Xiaoyong Chu, and Josef Pradler, “Simply split strongly interacting massive particles,” *Phys. Rev. D* **95**, 115023 (2017), [arXiv:1702.04906 \[hep-ph\]](#).
- [28] Juri Smirnov and John F. Beacom, “New Freezeout Mechanism for Strongly Interacting Dark Matter,” *Phys. Rev. Lett.* **125**, 131301 (2020), [arXiv:2002.04038 \[hep-ph\]](#).
- [29] Maxim Pospelov, “Particle physics catalysis of thermal Big Bang Nucleosynthesis,” *Phys. Rev. Lett.* **98**, 231301 (2007), [arXiv:hep-ph/0605215](#).
- [30] W. H. Breunlich, P. Kammel, J. S. Cohen, and M. Leon, “Muon-catalyzed fusion,” *Ann. Rev. Nucl. Part. Sci.* **39**, 311–356 (1989).
- [31] L. I. Ponomarev, “Muon catalyzed fusion,” *Contemp. Phys.* **31**, 219–247 (1990).
- [32] Martin Bauer and Tilman Plehn, *Yet Another Introduction to Dark Matter: The Particle Physics Approach*, Lecture Notes in Physics, Vol. 959 (Springer, 2019) [arXiv:1705.01987 \[hep-ph\]](#).
- [33] Edward W. Kolb and Michael S. Turner, *The Early Universe*, Vol. 69 (1990).
- [34] Kim Griest and Marc Kamionkowski, “Unitarity Limits on the Mass and Radius of Dark Matter Particles,” *Phys. Rev. Lett.* **64**, 615 (1990).
- [35] Nicolas Bernal, Camilo Garcia-Cely, and Rogerio Rosenfeld, “WIMP and SIMP Dark Matter from the Spontaneous Breaking of a Global Group,” *JCAP* **04**, 012 (2015), [arXiv:1501.01973 \[hep-ph\]](#).
- [36] N. Aghanim *et al.* (Planck), “Planck 2018 results. VI. Cosmological parameters,” *Astron. Astrophys.* **641**, A6 (2020), [arXiv:1807.06209 \[astro-ph.CO\]](#).
- [37] Bob Holdom, “Two U(1)’s and Epsilon Charge Shifts,” *Phys. Lett. B* **166**, 196–198 (1986).
- [38] Mauro Raggi and Venelin Kozhuharov, “Results and perspectives in dark photon physics,” *Riv. Nuovo Cim.* **38**, 449–505 (2015).
- [39] Martin Bauer, Patrick Foldenauer, and Joerg Jaeckel, “Hunting All the Hidden Photons,” *JHEP* **18**, 094 (2020), [arXiv:1803.05466 \[hep-ph\]](#).
- [40] Juebin Lao, Chengfeng Cai, Zhao-Huan Yu, Yu-Pan Zeng, and Hong-Hao Zhang, “Fermionic and scalar dark matter with hidden U(1) gauge interaction and kinetic mixing,” *Phys. Rev. D* **101**, 095031 (2020), [arXiv:2003.02516 \[hep-ph\]](#).
- [41] Marco Fabbrichesi, Emidio Gabrielli, and Gaia Lanfranchi, “The Dark Photon,” (2020), [arXiv:2005.01515 \[hep-ph\]](#).
- [42] E. C. G. Stueckelberg, “Interaction energy in electrodynamics and in the field theory of nuclear forces,” *Helv. Phys. Acta* **11**, 225–244 (1938).
- [43] Henri Ruegg and Marti Ruiz-Altaba, “The Stueckelberg field,” *Int. J. Mod. Phys. A* **19**, 3265–3348 (2004), [arXiv:hep-th/0304245](#).
- [44] Nikhil Padmanabhan and Douglas P. Finkbeiner, “Detecting dark matter annihilation with CMB polarization: Signatures and experimental prospects,” *Phys. Rev. D* **72**, 023508 (2005), [arXiv:astro-ph/0503486](#).
- [45] Silvia Galli, Fabio Iocco, Gianfranco Bertone, and Alessandro Melchiorri, “CMB constraints on Dark Matter models with large annihilation cross-section,” *Phys. Rev. D* **80**, 023505 (2009), [arXiv:0905.0003 \[astro-ph.CO\]](#).
- [46] Masahiro Kawasaki, Kazunori Nakayama, and Toyokazu Sekiguchi, “CMB Constraint on Dark Matter Annihilation after Planck 2015,” *Phys. Lett. B* **756**, 212–215 (2016), [arXiv:1512.08015 \[astro-ph.CO\]](#).
- [47] Hongwan Liu, Tracy R. Slatyer, and Jesús Zavala, “Contributions to cosmic reionization from dark matter annihilation and decay,” *Phys. Rev. D* **94**, 063507 (2016), [arXiv:1604.02457 \[astro-ph.CO\]](#).
- [48] N. Aghanim *et al.* (Planck), “Planck 2018 results. V. CMB power spectra and likelihoods,” *Astron. Astrophys.* **641**, A5 (2020), [arXiv:1907.12875 \[astro-ph.CO\]](#).
- [49] Junsong Cang, Yu Gao, and Yin-Zhe Ma, “Probing dark matter with future CMB measurements,” *Phys. Rev. D* **102**, 103005 (2020), [arXiv:2002.03380 \[astro-ph.CO\]](#).
- [50] O. Adriani *et al.* (PAMELA), “Cosmic-Ray Positron Energy Spectrum Measured by PAMELA,” *Phys. Rev. Lett.* **111**, 081102 (2013), [arXiv:1308.0133 \[astro-ph.HE\]](#).
- [51] M. Ackermann *et al.* (Fermi-LAT), “Searching for Dark Matter Annihilation from Milky Way Dwarf Spheroidal Galaxies with Six Years of Fermi Large Area Telescope Data,” *Phys. Rev. Lett.* **115**, 231301 (2015), [arXiv:1503.02641 \[astro-ph.HE\]](#).
- [52] A. Albert *et al.* (Fermi-LAT, DES), “Searching for Dark Matter Annihilation in Recently Discovered Milky Way Satellites with Fermi-LAT,” *Astrophys. J.* **834**, 110 (2017), [arXiv:1611.03184 \[astro-ph.HE\]](#).
- [53] M. Aguilar *et al.* (AMS), “Antiproton Flux, Antiproton-to-Proton Flux Ratio, and Properties of Elementary Particle Fluxes in Primary Cosmic Rays Measured with the Alpha Magnetic Spectrometer on the International Space Station,” *Phys. Rev. Lett.* **117**, 091103 (2016).

- [54] Stefano Profumo, Farinaldo S. Queiroz, Joseph Silk, and Clarissa Siqueira, “Searching for Secluded Dark Matter with H.E.S.S., Fermi-LAT, and Planck,” *JCAP* **03**, 010 (2018), [arXiv:1711.03133 \[hep-ph\]](#).
- [55] H. Abdallah *et al.* (HESS), “Search for γ -Ray Line Signals from Dark Matter Annihilations in the Inner Galactic Halo from 10 Years of Observations with H.E.S.S.” *Phys. Rev. Lett.* **120**, 201101 (2018), [arXiv:1805.05741 \[astro-ph.HE\]](#).
- [56] Xue-Lei Chen and Marc Kamionkowski, “Particle decays during the cosmic dark ages,” *Phys. Rev. D* **70**, 043502 (2004), [arXiv:astro-ph/0310473](#).
- [57] Sandeep Kumar Acharya and Rishi Khatri, “New CMB spectral distortion constraints on decaying dark matter with full evolution of electromagnetic cascades before recombination,” *Phys. Rev. D* **99**, 123510 (2019), [arXiv:1903.04503 \[astro-ph.CO\]](#).
- [58] Sandeep Kumar Acharya and Rishi Khatri, “CMB anisotropy and BBN constraints on pre-recombination decay of dark matter to visible particles,” *JCAP* **12**, 046 (2019), [arXiv:1910.06272 \[astro-ph.CO\]](#).
- [59] Masahiro Kawasaki, Kazunori Kohri, and Takeo Moroi, “Big-Bang nucleosynthesis and hadronic decay of long-lived massive particles,” *Phys. Rev. D* **71**, 083502 (2005), [arXiv:astro-ph/0408426](#).
- [60] Karsten Jedamzik, “Big bang nucleosynthesis constraints on hadronically and electromagnetically decaying relic neutral particles,” *Phys. Rev. D* **74**, 103509 (2006), [arXiv:hep-ph/0604251](#).
- [61] Masahiro Kawasaki, Kazunori Kohri, Takeo Moroi, and Yoshitaro Takaesu, “Revisiting Big-Bang Nucleosynthesis Constraints on Long-Lived Decaying Particles,” *Phys. Rev. D* **97**, 023502 (2018), [arXiv:1709.01211 \[hep-ph\]](#).
- [62] Kiyotomo Ichiki, Masamune Oguri, and Keitaro Takahashi, “WMAP constraints on decaying cold dark matter,” *Phys. Rev. Lett.* **93**, 071302 (2004), [arXiv:astro-ph/0403164](#).
- [63] Vivian Poulin, Pasquale D. Serpico, and Julien Lesgourgues, “A fresh look at linear cosmological constraints on a decaying dark matter component,” *JCAP* **08**, 036 (2016), [arXiv:1606.02073 \[astro-ph.CO\]](#).
- [64] Andreas Nygaard, Thomas Tram, and Steen Hannestad, “Updated constraints on decaying cold dark matter,” (2020), [arXiv:2011.01632 \[astro-ph.CO\]](#).
- [65] F. Bergsma *et al.* (CHARM), “A Search for Decays of Heavy Neutrinos in the Mass Range 0.5-{GeV} to 2.8-{GeV},” *Phys. Lett. B* **166**, 473–478 (1986).
- [66] J. D. Bjorken, S. Ecklund, W. R. Nelson, A. Abashian, C. Church, B. Lu, L. W. Mo, T. A. Nunamaker, and P. Rassmann, “Search for Neutral Metastable Penetrating Particles Produced in the SLAC Beam Dump,” *Phys. Rev. D* **38**, 3375 (1988).
- [67] M. Davier and H. Nguyen Ngoc, “An Unambiguous Search for a Light Higgs Boson,” *Phys. Lett. B* **229**, 150–155 (1989).
- [68] Johannes Blümlein and Jürgen Brunner, “New Exclusion Limits on Dark Gauge Forces from Proton Bremsstrahlung in Beam-Dump Data,” *Phys. Lett. B* **731**, 320–326 (2014), [arXiv:1311.3870 \[hep-ph\]](#).
- [69] M. Anelli *et al.* (SHiP), “A facility to Search for Hidden Particles (SHiP) at the CERN SPS,” (2015), [arXiv:1504.04956 \[physics.ins-det\]](#).
- [70] Jonathan L. Feng, Iftah Galon, Felix Kling, and Sebastian Trojanowski, “ForwArd Search ExpeRiment at the LHC,” *Phys. Rev. D* **97**, 035001 (2018), [arXiv:1708.09389 \[hep-ph\]](#).
- [71] Asher Berlin, Stefania Gori, Philip Schuster, and Natalia Toro, “Dark Sectors at the Fermilab SeaQuest Experiment,” *Phys. Rev. D* **98**, 035011 (2018), [arXiv:1804.00661 \[hep-ph\]](#).
- [72] P. H. Adrian *et al.* (HPS), “Search for a dark photon in electroproduced e^+e^- pairs with the Heavy Photon Search experiment at JLab,” *Phys. Rev. D* **98**, 091101 (2018), [arXiv:1807.11530 \[hep-ex\]](#).
- [73] Jae Hyeok Chang, Rouven Essig, and Samuel D. McDermott, “Revisiting Supernova 1987A Constraints on Dark Photons,” *JHEP* **01**, 107 (2017), [arXiv:1611.03864 \[hep-ph\]](#).
- [74] Jae Hyeok Chang, Rouven Essig, and Samuel D. McDermott, “Supernova 1987A Constraints on Sub-GeV Dark Sectors, Millicharged Particles, the QCD Axion, and an Axion-like Particle,” *JHEP* **09**, 051 (2018), [arXiv:1803.00993 \[hep-ph\]](#).
- [75] Allan Sung, Huitzu Tu, and Meng-Ru Wu, “New constraint from supernova explosions on light particles beyond the Standard Model,” *Phys. Rev. D* **99**, 121305 (2019), [arXiv:1903.07923 \[hep-ph\]](#).
- [76] Eric Kuflik, Maxim Perelstein, Nicolas Rey-Le Lorier, and Yu-Dai Tsai, “Elastically Decoupling Dark Matter,” *Phys. Rev. Lett.* **116**, 221302 (2016), [arXiv:1512.04545 \[hep-ph\]](#).
- [77] Duccio Pappadopulo, Joshua T. Ruderman, and Gabriele Trevisan, “Dark matter freeze-out in a nonrelativistic sector,” *Phys. Rev. D* **94**, 035005 (2016), [arXiv:1602.04219 \[hep-ph\]](#).
- [78] Marco Farina, Duccio Pappadopulo, Joshua T. Ruderman, and Gabriele Trevisan, “Phases of Cannibal Dark Matter,” *JHEP* **12**, 039 (2016), [arXiv:1607.03108 \[hep-ph\]](#).
- [79] Eric Kuflik, Maxim Perelstein, Nicolas Rey-Le Lorier, and Yu-Dai Tsai, “Phenomenology of ELDER Dark Matter,” *JHEP* **08**, 078 (2017), [arXiv:1706.05381 \[hep-ph\]](#).
- [80] Patrick J. Fitzpatrick, Hongwan Liu, Tracy R. Slatyer, and Yu-Dai Tsai, “New Pathways to the Relic Abundance of Vector-Portal Dark Matter,” (2020), [arXiv:2011.01240 \[hep-ph\]](#).
- [81] Chuan-Yang Xing and Shou-hua Zhu, In preparation.